CDF/DOC/BOTTOM/CDFR/6345
May 22, 2003
Version 1.0

Study of B_s yields in the hadronic trigger

Donatella Lucchesi, Saverio Da Ronco,
INFN Padova and Università di Padova, Padova, Italy
Alessandro Cerri,
Laurence Berkeley National Laboratory, Physics Division, Berkeley-Ca, USA
S. De Cecco, S. Giagu, M. Rescigno,
INFN Roma1 and Università di Roma "La Sapienza", Roma, Italy
R. Carosi, S. Donati, G. Punzi, D. Tonelli,
INFN Pisa, Università and Scuola Normale di Pisa, Padova, Italy
S. D'Auria,
Glasgow University, Glasgow United Kingdom
M. Campanelli
University of Geneva, Geneva, Switzerland

Abstract

Understanding the B_s yield in the two track trigger is of primary importance in view of the Run 2 mixing frequency measurement.
In this note we measure the $B_s \to D_s^{\mp}\pi^{\pm}$ yield relative to $B_d \to D^{\mp}\pi^{\pm}$ and we check the detector and trigger simulation by comparing the $B_d \to D^{\mp}\pi^{\pm}$ with the $B_u \to D^0\pi^{\pm}$ yield where all the branching ratios are known and the uncertainty on f_d/f_u is negligible. After correcting for the relative detector, trigger and reconstruction effects we measure

$$\frac{f_s}{f_d}\frac{Br(B_s \to D_s\pi)}{Br(B_d \to D\pi)} = 0.42 \pm 0.11(stat.) \pm 0.11(BR) \pm 0.07(syst.)$$

1 Introduction

In the Tevatron yellow book [6], in [7] and [5] we gave a crude estimate of what CDF expected to achieve in terms of B_s yields exploiting the innovative secondary vertex trigger.
Now we have enough data to verify those expectations and the assumptions they were based on: initially we found out that the B_d yield was lower than expected, and had predictions for what the B_s yield should have been in more stable running conditions.

After more than 1 year of stable data taking we know that the initial expectations were rather optimistic, but on the other hand we now have a sound understanding of how to correctly give estimates on these yields and indications on what we can do to recover the B physics reach we expected to achieve in Run IIa.

Since absolute estimates are much harder to produce, and necessarily involve absolute cross section measurements, we concentrate our effort on the measurement of *relative* yields, comparing the observed number of events for $B_s \to D_s^{\mp}\pi^{\pm}$, $B_d \to D^{\mp}\pi^{\pm}$, and $B_u \to D^0\pi^{\pm}$.

We think that this both gives the opportunity of evaluating our B physics reach, but also opens new perspectives on the possibility of directly measuring important phenomenological quantities (namely f_s/f_d) once we will establish a good understanding of the trigger and detector acceptances.

This note is structured in the following way:

- Section 2 describes the data sample on which the rest of the note is based and the reconstruction which is common to the three decays;

- In section 3 we describe the B_s reconstruction: the cuts used are studied on Monte Carlo and optimized for high signal efficiency;

- section 4 is devoted to the reconstruction of $B_d \to D^{\mp}\pi^{\pm}(D \to K\pi\pi)$.
  We choose on purpose to use the same cuts applied on the B_s signal in order to simplify the interpretation of the relative yields;

- In section 5 the decay $B^{\pm} \to D^0\pi^{\pm}$ is reconstructed as well;

- Section 6 deals with the evaluation of the relative trigger and reconstruction efficiencies. This study is based on the *realistic* Monte Carlo, i.e. a full geant simulation of the CDF II detector followed by the emulation of the trigger selection;

- In the last section (sec. 7) we compare all the numbers and evaluate the yields.

2 Data Sample

The sample used in this study is the full `hbot0h` dataset available as a static sample in the CAF facility. This corresponds to $\approx 64\,pb^{-1}$ of *multi-body* two track trigger data after the following requirements:

- using the `prereq` module to insure that the only trigger path being analyzed are `B_CHARM` variants (namely `B_CHARM_LOWPT`, `B_CHARM`, `B_CHARM_HIGHPT`)
- "Bad runs" are excluded according to the most recent insight of the validation subgroup [3]

All the current recommendations given by the B group for reconstruction are followed. In particular we base our analysis on `cdfsoft 4.9.1` and re-fit tracks with the following options:

- Drop L00 and ISL hits;
- Re-fit using the KAL re-fitter;
- Re-scale the COT covariance matrix with the scale factors $(c, d_0, \phi_0, z_0, \lambda) = (5.33, 3.01, 3.7, 0.653, 0.58)$;
- Alignment table `100030 1 GOOD`;

Signals are reconstructed using `CharmMods` [2], always requiring for each track 20+20 (Axial+Stereo) COT hits and 3 $r-\phi$ silicon hits in any part of the detector *before re-fitting* . Any track is required to satisfy at least $P_t > 0.5\,GeV$ and $|\eta| < 2$.

The primary vertex is found using the beam line position. For each event the position of the beam in x_0, y_0 and its slopes $(dx/dz,\ dy/dz)$ relative the standard CDF system of coordinates are retrieved from the database. We explicitly require these quantities to be based on silicon vertex information. The primary vertex position is then :

$$x_{PV} = x_0 + \frac{dx}{dz} \cdot z_{PV}$$
$$y_{PV} = y_0 + \frac{dy}{dz} \cdot z_{PV}$$

where z_{PV} is calculated averaging the z_0 of all tracks in the candidate.

3 B_s reconstruction

The B_s is reconstructed through the decay $B_s \to D_s\pi$ with $D_s \to \phi\pi$ and $\phi \to K^+K^-$. We keep the selection as simple as possible, in order to simplify the understanding of the relative efficiencies. We require the trigger confirmation for 2 out of 4 tracks of the candidate: offline tracks are associated to the SVT applying loose matching requirements in $(\Delta c, \Delta\phi_0)$. The cuts on impact parameter, transverse momentum, $\Delta\phi$ and opposite charge are applied to the SVT quantities, no L_{xy} and $P_t^1 + P_t^2$ are requested. The following analysis cuts are tuned on the realistic Monte Carlo simulation of the

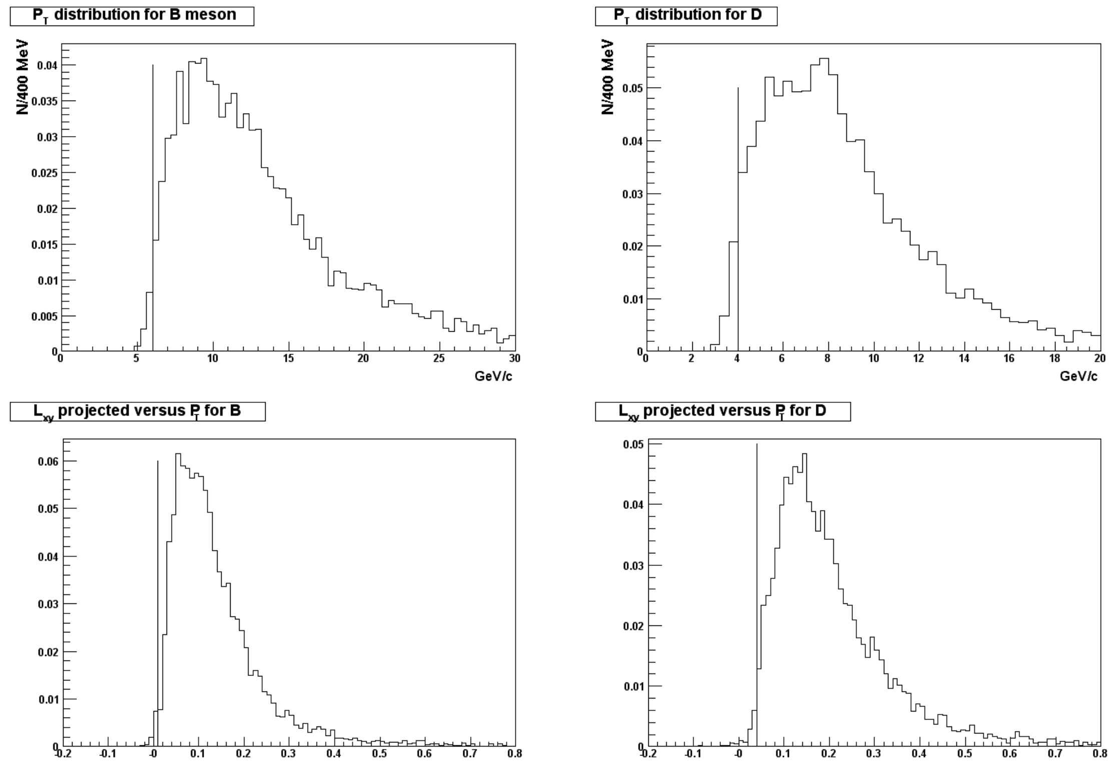

Figure 1: Top: Transverse momentum of the reconstructed B_s (left); transverse momentum of the reconstructed D_s (right). Bottom: B_s decay length projected into the B_s transverse momentum on the left and D_s decay length projected into the D_s transverse momentum respect to the primary vertex on the right.

signal selected by the standard *scenario A* two tracks trigger conditions [4] so that each cut is $O\,(90\%)$ efficient on the signal:

1. The D_s and B_s are reconstructed using `CTVMFT`;
2. $m\,(K^+K^-) \in [1.013, 1.028]\ GeV$;
3. The D_s mass is constrained to the PDG value;
4. $\Delta R\,(D_s\pi_B) < 1.5$ (where π_B is the pion coming from the B);
5. $\chi_{xy}^{B_s} < 15$, $\chi_{xy}^{D_s} < 10$;

6. $P_t^{D_s} > 4GeV$ and $P_t^{B_s} > 6GeV$;

7. $L_{xy}^{D_s} > 400\mu m$, $L_{xy}^{B_s} > 100\mu m$
where each $L_{xy}^X = \vec{P}_t^{yy} \cdot (\vec{X}_{yy} - \vec{X}_{PV})$ is calculated with respect to the primary vertex ($\vec{X}_{PV}$);

8. The impact parameter for the fully reconstructed B_s meson is required to satisfy $|d_{B_s}| < 100\mu m$.

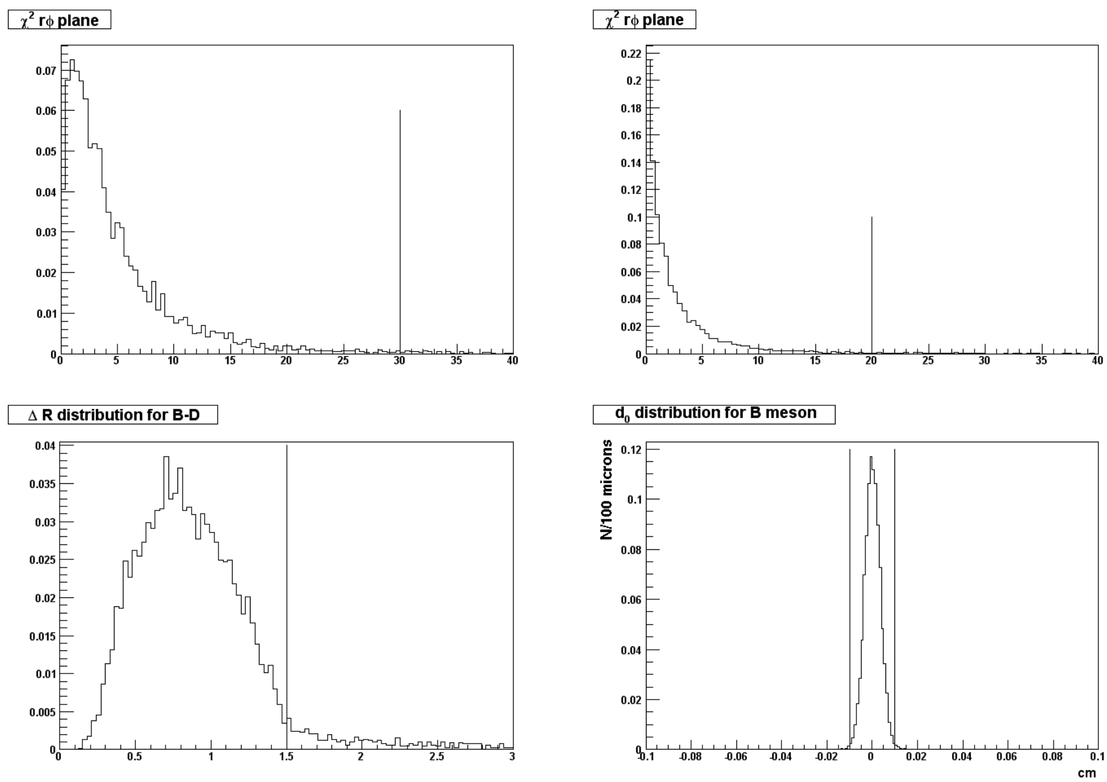

Figure 2: Top:Bidimensional (r, ϕ) χ^2 distribution for the B_s vertex (left) and the D_s vertex (right). Bottom: Delta R between the D_s direction and the pion coming from the B(left) B impact parameter respect to the primary vertex(right).

We decide to not optimize the cuts by requiring the best signal to noise ratio mainly for two reasons. The first one is that the number of candidates is quite low and we risk to optimize cuts on statistic fluctuations. The second one comes from the physics itself, it is very difficult to find an unbiased background sample. We can not use the B_s side bands since they have the $B_s \to D_s^* \pi$ contribution as it will be evident later. One can argue that we should use the $B_d \to D^{\mp}\pi^{\pm}$ where the statistics is high and there are well defined side bands. However, the two signals are different even if they have the same multiplicity in the final state: in particular the B_s mode can be cleaned up thanks to the narrow intermediate resonance ($\varphi \to KK$), whereas the same handle is not present in the B_d decay. We therefore privilege the strategy of leaving the cuts very simple and quite loose. For instance, we follow a loose optimization only for the two χ^2 cuts on the large statistics sample (B_d) and then we transport them without further optimization to the B_s signal.

As a reference we report in figures 1 and 2 the distribution of the discriminating variables for a full simulation of pure signal where the $B_s \to D_s\pi$ and $D_s \to \varphi\pi$ and $\varphi \to KK$ decays are forced. The configuration used for these montecarlo events will be described later in section 6. The events are then reconstructed just like regular data and then tracks are re-fit dropping L00 and ISL hits but without scaling the track covariance matrix. We learned too late, that this is a mistake since also the Monte Carlo covariance matrix needs to be rescaled.

Kinematic quantities, like the transverse momentum or the angles between the decay products are known to be well reproduced by the Monte Carlo. We double check the impact parameter and the decay length distributions, which are critical to our analysis and are closely dependent on the trigger bias and detector resolution uncertainties. These checks will be done by using an high statistic sample and described in section 6.

The cut on the two kaons invariant mass is determined by looking at the data. In figure 3 this distribution is shown with the two vertical lines indicating the applied cuts which correspond to -2σ, $+3\sigma$. We decided to apply an asymmetric cut around the peak because of the asymmetric background.

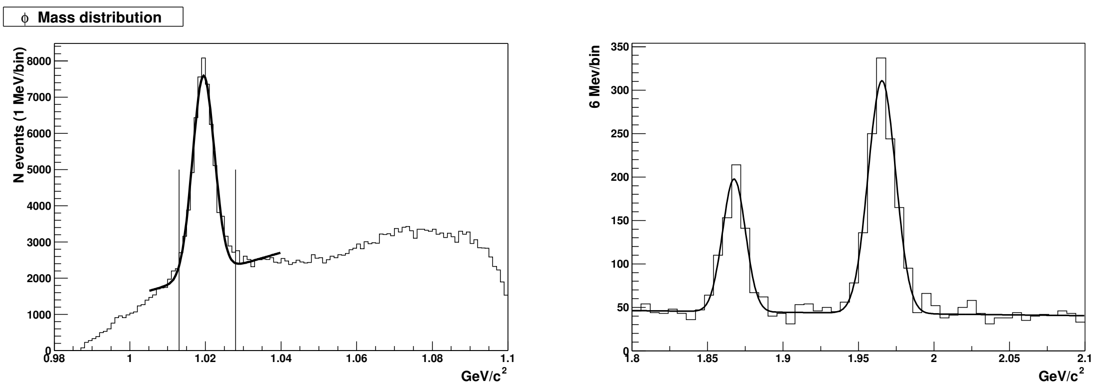

Figure 3: Left: φ invariant mass distribution for all the combinations which pass trigger confirmation and χ^2 cuts. The fitted mass is 1.01946 ± 0.00002 GeV/c^2 and the width $\sigma = 2.88 \pm 0.03$ MeV/c^2. Right: $\varphi\pi$ invariant mass distribution. The fitted parameter are summarized in the text.

The B_s is reconstructed by applying a mass constrained fit of the D_s to the PDG value. We check that this is not introducing a bias removing the constraint.

The fitted values for the D_s mass (figure 3) are:

	Mass (MeV/c^2)	Width (MeV/c^2)
$D^\pm$	1867.7 ± 0.5	7.6 ± 0.5
D_s	1966.0 ± 0.4	9.0 ± 0.4

Before looking at the data we applied all the cuts described above to the Monte Carlo. The result of this procedure on the Monte Carlo is shown in figure 4 where the invariant mass distribution of the candidates for the forced Monte Carlo is reported (left) after all cuts. The mean is 5.336 ± 0.001 GeV and the width 19.0 ± 0.6 MeV. As further

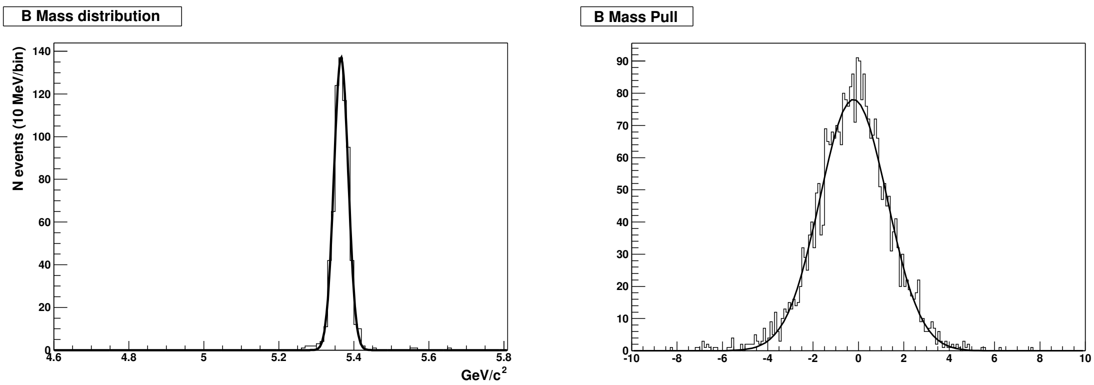

Figure 4: Invariant mass distribution of the candidates $B_s \to D_s\pi$, $D_s \to \phi\pi$, $\phi \to KK$ in a full geant simulation of the detector+trigger conditions on the sole signal (left) and its pull on the right..

check that the mass constraint fit does not bias the invariant mass distribution we plot on figure 4 (right) the B mass pull, its mean is slightly negative(-0.2) and the width is 1.4, considering that we do not scale the covariance matrix this result is within the expectations.

Since we can in principle have a significant contribution from fully reconstructed D_s from other sources, we generate an high statistics sample of inclusive single B decays with `BGenerator` and select those events passing the trigger requirements which in addition contain a generator level D_s particle. All D_s in this sample are forced to decay according to the chain: $D_s \to \phi\pi$, $\phi \to KK$.
Figure 5(left) reports the invariant mass distribution for the candidates in this sample: this will provide an useful template when we try to understand the distribution seen on data.

We fit the inclusive D_s Monte Carlo invariant mass distribution. The model used is exponential for the background in addition to two Gaussian components, corresponding to the direct decay $B_s \to D_s\pi$, $D_s \to \phi\pi$, $\phi \to KK$ and to the partially reconstructed $B_s \to D_s^*\pi$, $D_s^* \to D_sX$, $D_s \to \phi\pi$, $\phi \to KK$. The fit results are summarized in the

Configuration	$N^o_{B_s(D_s)}$	$N^o_{B_s(D_s^*)}$	$B_s(D_s)$ mass [GeV]	$B_s(D_s)$ σ [MeV]	$B_s(D_s^*)$ mass [GeV]	$B_s(D_s^*)$ σ [MeV]
MC	169±14	282± 43	5.366 ± 0.002	17 ± 1	5.139 ± 0.008	77 ± 5
Different range	178±14	276±31	5.366 ± 0.002	18 ± 1	5.144 ± 0.07	71 ± 7
HepG	170	234				

Table 1: Fit results on Monte Carlo with an exponential+bi-gaussian model for the background and the two signal components described in the text. The second part of the table refers to the systematics studies reported in the text.

table 1. The number of events returned by the fit is in quite good agreement with what is in the HepG banks ($N^{mc}_{B_s(D_s)}$=170 and $N^{mc}_{B_s(D_s^*)}$=234). The fit returns a ratio $N^o_{D_s^*\pi}/N^o_{D_s\pi}$=1.3 ± 0.2. This number is within statistics compatible with the value fed to the montecarlo generator for the relative contribution (1.3) as well as with the montecarlo *truth* based on the generator information (1.4 ± 0.1).

We need to asses the systematics coming also from the particular choice of the fit range that we are proposing. Fitting the $D_s\pi$ invariant mass distribution in a shorter range [4.9, 5.4] with the same background parameterization we obtain a larger number of B_s for both peaks, still consistent however with the information in the HEPG bank. The two fit options bracket the true value and are both quite stable.

The Monte Carlo distribution provides a model to test the parameterization of the invariant mass distribution used to fit the data. However the montecarlo does not contain all the background components: tracks from the opposite side b as well as those from the underlying event are not modeled at all. The distribution in the left of figure 5 suggests however that the data is modeled rather well with the simplistic assumption that all candidates contain a real reconstructed D_s from a $B_{u,d,s}$ decay plus a low combinatorial background.

The same fit model is thus applied to the data, as shown in figure 5 (right). The results are summarized in table 2. In order to check the stability of the fit procedure we then vary the background model from an exponential to a quadratic polynomial form (BCK 1). The fit returns the same number of B_s events while the contribution of the D_s^* is less evident but still compatible within errors.
We then apply to the data the test already done on Monte Carlo: a fit in a restricted range. The size of the resulting variation is still compatible to the one observed in the MC, even if additional background seems to significantly perturbate the fit. We can conclude that we know rather well how to extract the effective B_s yield from the reconstructed sample. This requires the use of a realistic model for the satellite peak coming from partly reconstructed D_s^* decays, even if the additional events aren't included in the yield studies.

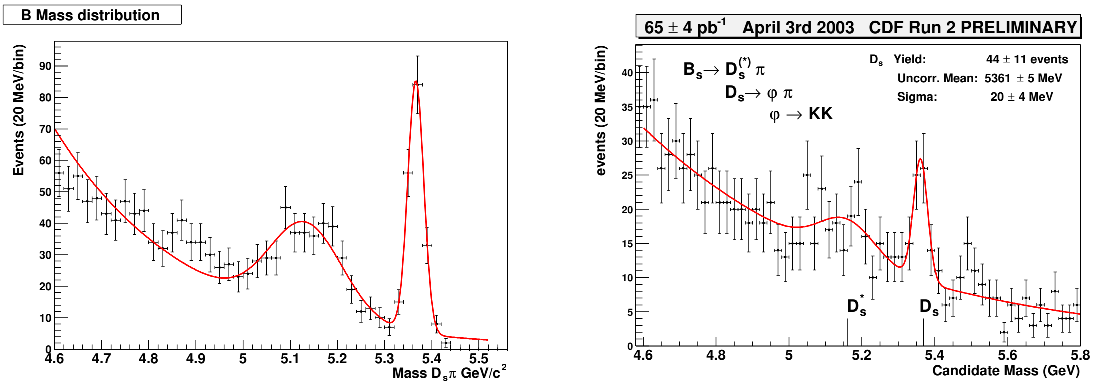

Figure 5: Data invariant mass distribution of the candidates $B_s \to D_s\pi$, $D_s \to \phi\pi$, $\phi \to KK$ on sample composed of generic single $B_{u,d,s}$ decays containing at least one D_s particle in the generator level decay(left) and data (right).

Configuration	$\mathrm{N}^o_{B_s(D_s)}$	$\mathrm{N}^o_{B_s(D_s^*)}$	$B_s(D_s)$ mass [GeV]	$B_s(D_s)$ σ [MeV]	$B_s(D_s^*)$ mass [GeV]	$B_s(D_s^*)$ σ [MeV]
Data all cand.	44±11	53 ± 21	5.361 ± 0.005	20 ± 5	5.16 ± 0.03	77 ± 27
Data BCK1	44±10	36±18	5.360 ± 0.006	22 ± 6	5.15 ± 0.04	64 ± 28
Different range	36±11	43±30	5.360 ± 0.005	17 ± 6	5.14 ± 0.04	69 ± 32

Table 2: Fit results on data with an exponential+bi-gaussian model for the background and the two signal components described in the text. The second row of the table refers to the systematics study done varying the background parameterization, and the third shows the results for the change of the fit range.

4 B_d Reconstruction

As a reference sample for direct comparison with the B_s decay we choose $B_d \to D^{\mp}\pi^{\pm}$, $D^{\mp} \to K^{\mp}\pi^{\pm}\pi^{\mp}$. This decay mode has the advantage of sharing the same final state multiplicity and a sufficiently close kinematics to $B_s \to D_s\pi$, $D_s \to \phi\pi$, $\phi \to KK$. Measuring the relative branching fraction between these B_s and B_d modes gives a smaller sensitivity to systematics coming from a non perfect reproduction of the detector and trigger conditions (e.g. the SVX II coverage or the single hit detection efficiency).
Again in the spirit of gaining independence on such systematics we pick a set of selection cuts as close as possible to the B_s case.
The trigger confirmation is the same used for B_s: two out of the four offline tracks used must be associated to SVT tracks and the transverse momentum, the impact parameter the charge and the ϕ angle between these tracks have to satisfy the scenario

A trigger requirements. The analysis cuts then are (keeping a numbering scheme as close as possible to the one used for the B_s selections):

1. The $D^{\pm}$ and B_d are reconstructed using `CTVMFT`;
2.
3. The $D^{\pm}$ mass is constrained to the PDG value;
4. $\Delta R\,(D^{\pm}\pi_B) < 1.5$ (π_B is the pion coming from the B);
5. $\chi^{B_d}_{xy} < 15$, $\chi^{D^{\pm}}_{xy} < 10$;
6. $P_t^{D^{\pm}} > 4\ GeV$ and $P_t^{B_d} > 6\ GeV$;
7. $L^{D^{\pm}}_{xy} > 600\mu m$, $L^{B_d}_{xy} > 100\mu m$
   where each $L^{X}_{xy} = \vec{P}_t^{yy} \cdot (\vec{X}_{yy} - \vec{X}_{PV})$ is calculated with respect to the primary vertex ($\vec{X}_{PV}$);
8. The impact parameter for the fully reconstructed B_d meson is required to satisfy $|d_{B_d}| < 100\mu m$.

The main differences between this decay and the B_s are, beside the absence of cuts on the $\varphi \to KK$ decays, in the angle between π_B and the D as well as the D decay length. In the left of figure 6 we show the $\Delta R\,(\pi_B - D)$ for B_d (full line) and B_s decays (dashed line). The two distribution have the same behavior and cutting at 1.5 it is safe for both. On the right of figure 6 we see the $D^{\pm}$ (full line) and D_s (dashed line) decay length distributions. The vertical line shows where we cut for B_s. The fact that the $D^{\pm}$ lifetime is longer than D_s lifetime is evident from the plot. This explains why we will find a relative trigger efficiency which slightly favors the B_d events (see section 6).
We choose a rather conservative lower cut of 600 μm for this decay length. The effect of the different lifetime is taken into account in the efficiency as well as a source of systematic error (sections 6). As we discussed already, the cuts on χ^2_B and χ^2_D are loosely optimized on this sample. The optimization is performed fixing all the other analysis cuts to the nominal values and then floating the cuts on $\chi^{B_d}_{xy}$ and $\chi^{D^{\pm}}_{xy}$. Figure 7 summarizes the results of this stdy in terms of the $S/\sqrt{S+B}$ dependancy on each of the two quantities when cutting at the nominal value for the other one. The final choice is tha of cutting at 10 for the D component and 15 for the B overall χ^2.

After the Monte Carlo data is processed with the same code and after applying all the reconstruction cuts, we end up with an invariant mass distribution (figure 8, left) which has a width of 18.4 ± 0.6 MeV. Since also in this case we apply a mass constraint on the $D^{\pm}$ mass we cerify that the bias on the B invariant mass distribution is negligible. In figure 8, right we plot the mass pull: the mean is -0.11 ± 0.06 and

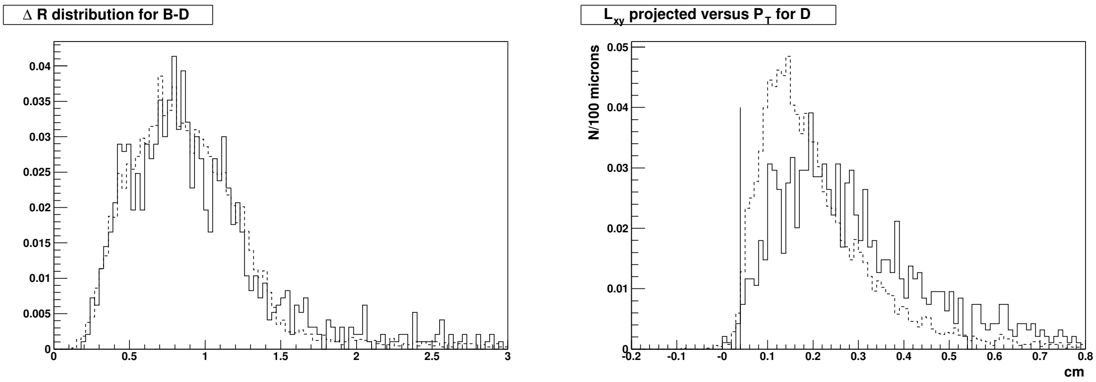

Figure 6: Left: ΔR for B_d (full line) and for B_s (dashed line). Right: decay length for $D^{\pm}$ (full line) and D_s (dashed line).

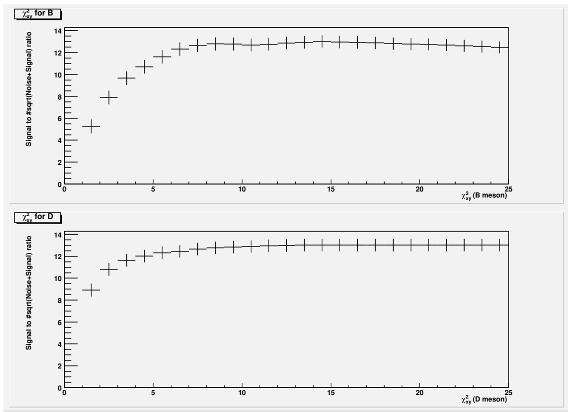

Figure 7: $S/\sqrt{S+B}$ distributions varing the χ^2 cut.

the sigma 1.42 ± 0.05. This is consistent with the expectations, given the fact that we are not correcting the covariance matrix errors.

As double check we also reconstruct the $B_d \rightarrow D^{\mp}\pi^{\pm}$ on data without the mass constraint, the result is shown in figure 9. On the left we report the $K\pi\pi$ invariant mass distribution for the $D^{\pm}$ candidates, while on the right we plot the $K\pi\pi\pi$ invariant mass which shows the B_d signal and the contribution of the partially reconstructed decays. The number of events returned from the fit is 506 ± 50 the mean is 5.265 ± 0.003 GeV and the width 27 ± 2 MeV. The lower mass peak contains 208 ± 50 events, with a mean of 5.019 ± 0.006 GeV and is 24 ± 6 MeV wide.

The data with the mass constraint is shown in figure 10 (left) with the fit superimposedl the fit results are summarized in table 3.

The fit model in this case is less controversial than for the B_s case, since the peak has no so close neighboring resonance and the background has a milder behavior. Nevertheless we cross check this producing a generic $B_{u,d,s}$ Monte Carlo where we

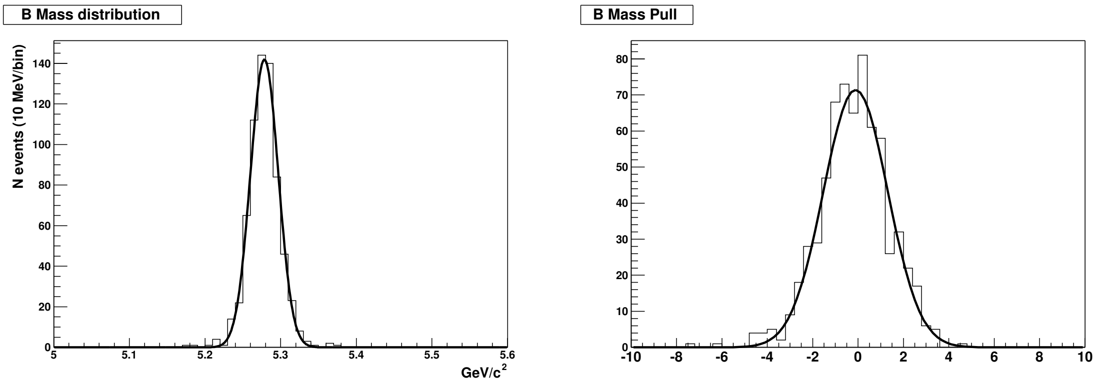

Figure 8: Left: Invariant mass distribution for the forced Monte Carlo. Right: Pull distribution for the reconstructed mass minus the PDG value divided by the error returned by the fit.

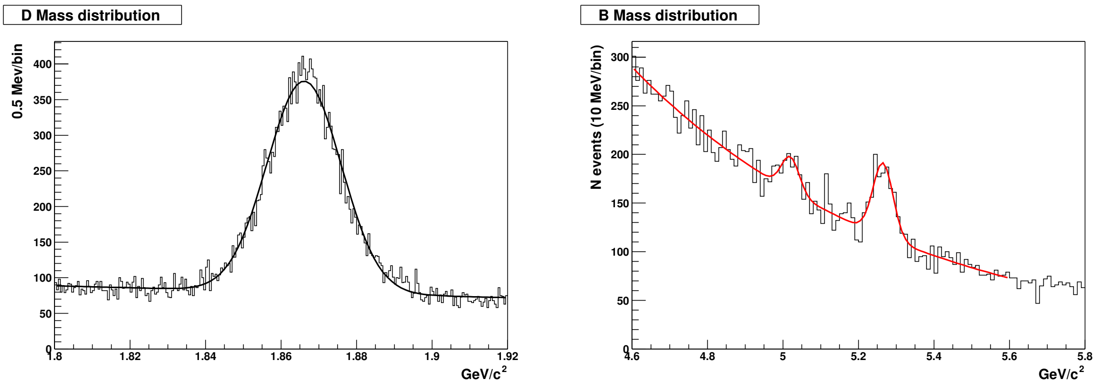

Figure 9: Left: $K\pi\pi$ invariant mass distribution for all the combinations and for all the B_d candidate. Right: $K\pi\pi\pi$ invariant mass distribution without the mass constraint on the $D^{\pm}$.

force $D^{\pm} \to K\pi\pi$. We then filter the events asking for at least one $D^{\pm}$ in the event at generation level. In figure 10 (right) the invariant mass of this Monte Carlo after all the reconstruction and analysis cuts is shown. The Monte Carlo plot confirms that our model for the background is correct.

Configuration	N events	Mass GeV	σ MeV
N^o $B^0(D^{\pm})$	505 ± 44	5.267 ± 0.002	23 ± 2
N^o $B^0(D^{\pm *})$	237 ± 48	5.023 ± 0.005	24 ± 5

Table 3: Results of the fit to the $B_d \to D^{\mp}\pi^{\pm}$ candidates. See text for details.

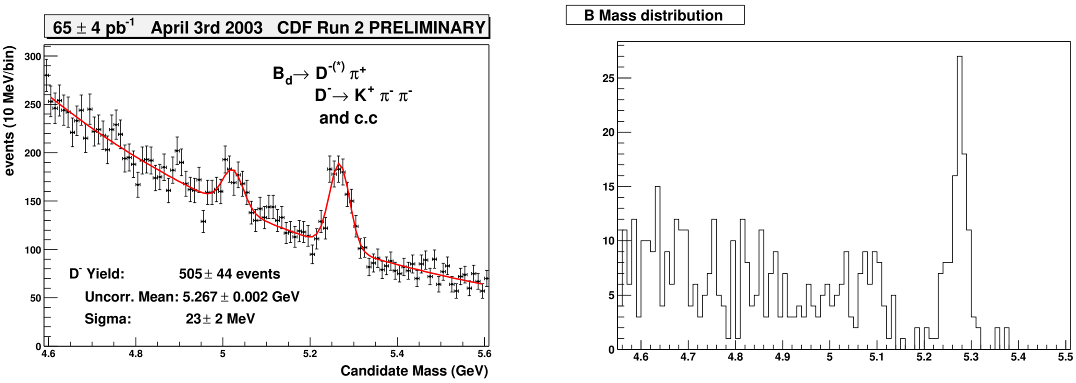

Figure 10: Invariant mass distribution for the reconstructed $B \to D^{\pm}\pi^{\mp}$ candidates, with a superimposed Gaussian+exponential background fit. The left plot shows the real data, while the right plot reports the full Monte Carlo.

5 $B^{\pm}$ reconstruction

Reconstructing another signal and measuring a better known relative yield is an important cross check of the detector and trigger simulation. This is why we perform a yield comparison against the simulation which does not involve the uncertainty on f_s/f_d.
In the previous version of this note we used the $B^{\pm} \to J\psi K^{\pm}$ as demonstration that the Monte Carlo reproduces the data with sufficient accuracy for the measurement we want to do.

The reconstruction of $B^{\pm} \to J\psi K^{\pm}$ presents however several problems, which involve an intrinsic understanding of the detector performances. Our reconstruction was solely based on tracking, disregarding any form of muon or electron identification. Both $J/\Psi \to ee$ and $J/\Psi \to \mu\mu$ contribute to the sample with a different efficiency (due to the different behavior of muon and electrons in our detector). The presence of candidates with electrons in the final state increases the uncertainty with which we can estimate this signal's yield in the simulation.
To avoid this we switcht o another decay, $B^{\pm} \to D^0\pi^{\pm}$ (with $D^0 \to K\pi$). Like the $B^{\pm} \to J\psi K^{\pm}$ this decay has 3 tracks in the final state whereas our reference decays have 4. Any comparison with the and B_d decays has to take into account this extra (in)efficiency which for the moment is evaluated from the Monte Carlo .
We will see, however, that the difference in efficiency is not affecting significantly the conclusions of our study.

The signal reconstruction is still done using `CharmMods` and the standard tracks reconstruction procedure already outlined. The trigger confirmation is still the same used before and the analysis cuts applied are:

1. The and B_u is reconstructed using `CTVMFT`;

2.

3. The D^0 mass is constrained to the PDG value;

4. $\Delta R\,(D^0\pi_B) < 1.5$;

5. $\chi^{B_u}_{xy} < 15$, $\chi^{D^0}_{xy} < 10$;

6. $P_t^{D^0} > 4GeV$ and $P_t^{B_u} > 6GeV$;

7. $L^{D^0}_{xy} > 400\mu m$, $L^{B_u}_{xy} > 100\mu m$
   where each $L^X_{xy} = \vec{P}_t^{yy} \cdot (\vec{X}_{yy} - \vec{X}_{PV})$ is calculated with respect to the primary vertex $(\vec{X}_{PV})$;

8. The impact parameter for the fully reconstructed B_u meson is required to satisfy $|d_{B_u}| < 100\mu m$.

The invariant mass fit presents some issue due to the irregular shape of the satellite peaks (see left of figure 11). We produce a large sample of Monte Carlo in the attempt to reproduce these features, but the combinatorial background here seems to play an important role and may require the use a full $b\bar{b}$ Monte Carlo.

On the left of figure 11 we show the invariant mass distributions for all candidates, and on the right the same distribution for Monte Carlo. The fit model is two Gaussian for the signal and an exponential for the background. The results of the fits are summarized in the table 4. The model used is not describing very well the satellite peak. We assume the presence of only one peak while it is evident that there is a substructure in the satellite. Further studies to fit the 2 peaks woould need a more accurate and statistically significant Monte Carlo, but we think that this is not going to significantly affect the determination of the number of $B_u \to D^0\pi^\pm$.

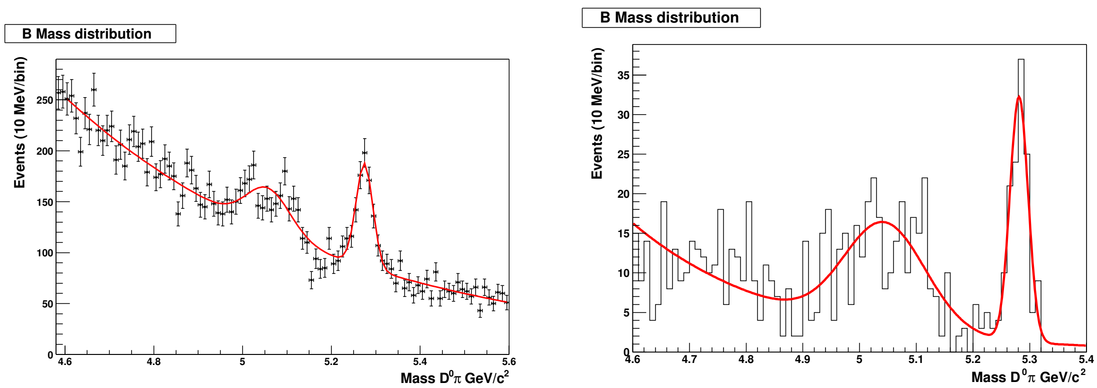

Figure 11: Invariant mass distribution for the reconstructed $B^\pm \to D^0\pi^\pm$ candidates, with a superimposed bi- Gaussian+exponential background fit. The left plot shows the data, while the right plot reports the Monte Carlo.

Configuration	N events	Mass GeV	σ MeV
All candidates	485 ± 42	5.274 ± 0.002	19 ± 2
Second peak	519 ± 66	5.058 ± 0.007	49 ± 5

Table 4: Results of the fit to the $B_u \to D^0\pi^{\pm}$ candidates. See text for details.

6 Efficiencies evaluation

6.1 Detector and Trigger Effects

The data CDF has at the moment was taken under several different conditions: partial coverage of the silicon, inefficient SVT patterns, high and low luminosity (with the corresponding changes to the trigger scenario). Our goal is that of averaging out all these effects and obtain for each decay mode a luminosity-weighted average of the data taking configuration. This is far from being simple and well established.
Measuring relative efficiencies makes our task easier, but in any case there will be systematic effects due to the configuration changes.
For this reason a procedure for *detailed* Monte Carlo simulation has been developed which can in principle take into account detector and trigger configuration changes. This simulation is still not completely faithful, and inaccuracies have to be accounted for as additional systematic errors, but it has been proven to give an overall decent reproduction of the running conditions.
The detailed Monte Carlo is based on a full geant simulation of the detector and an accurate emulation of the trigger configuration. However, in order to simplify the simulation task, we will take one representative run configuration as the baseline for our studies, preliminarly evaluating the run-dependent configuration changes as an additional source of systematics.
We used `Bgenerator` to generate one single B mesons, the decay is handled by `EvtGen` while the detector and trigger systems are simulated by `CdfSim` and `TrgSim++`. We generated two different samples of Monte Carlo events. One with high statistic where the minimum b quark momentum is required to be grater than 5.5 GeV and $|y| < 1.3$. This is the sample used to evaluated the central value for the efficiency ratios. Since this cut can introduce a potentially significant bias, we assess the systematics coming from this cut generating a second sample with a minimum b quark momentum of 0 and evaluate the effect of the cut at 5.5 in the previous generation.

The detector and trigger simulation has been generated for 8 different run conditions, which take into account eight different periods of data taking. Each of these periods is identified by consistent running conditions and significantly differs from the other ones. In table 5 these run ranges are reported with an explanation of the relevant

Run Ranges	Luminosity(pb^{-1}	Comment
138809-143000	3.4	Scenario A implemented
143001-146000	3.7	Tevatron incident
146001-149659	7.2	SVX coverage improved
149660-150009	0.6	SVT optimization (coverage+patterns)
150010-151117	1.9	$L_{xy} > 200$ μm for `B_PIPI`
151118-152668	10.7	Scenario A to B + DPS
152669-152952	2.3	XFT 1 miss
152953-155409	34.	Scenario B to C + DPS

Table 5: Range of runs from where we selected our run to simulated a particular detector condition.

differences with the preceding ranges.

XFT and SVT cuts do vary as well along these run ranges, in the sense that the L2 requirements on the trigger objects differ as well. We will eventually take into account these differences as additional systematic sources.

Before using this Monte Carlo to evaluate the efficiencies we want to gain confidence in its ability of reproducing the data distributions for critical quantities like impact parameter and decay lengths. In figure 12 we compare the impact parameter of the

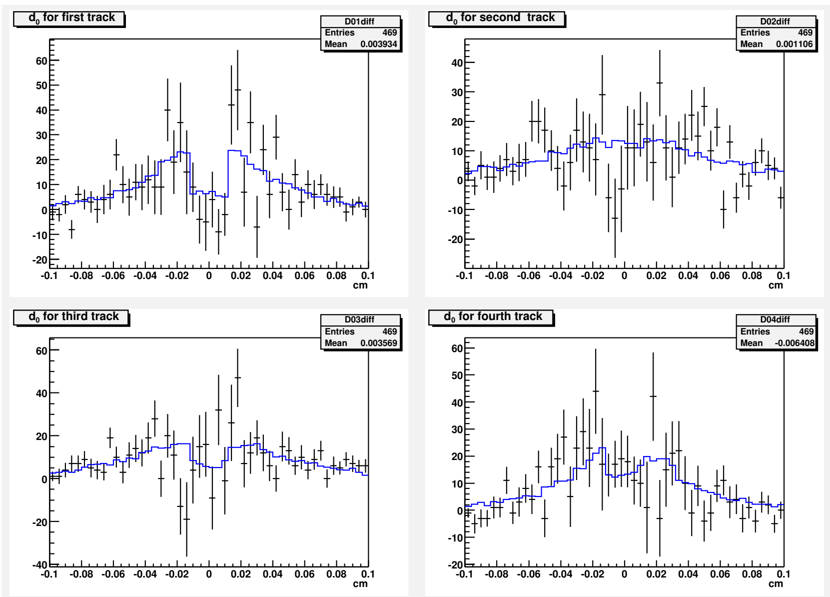

Figure 12: Comparison between Monte Carlo simulation and Data.

tracks for the $B_d \rightarrow D^{\pm}\pi^{\mp}$ decay. The Monte Carlo is a sample generated at $P_t^b = 0$

(blue line in the histograms) and is overlayed to the sideband subtracted data (black dots). The good agreement between data and MC is confirmed also in the B and D

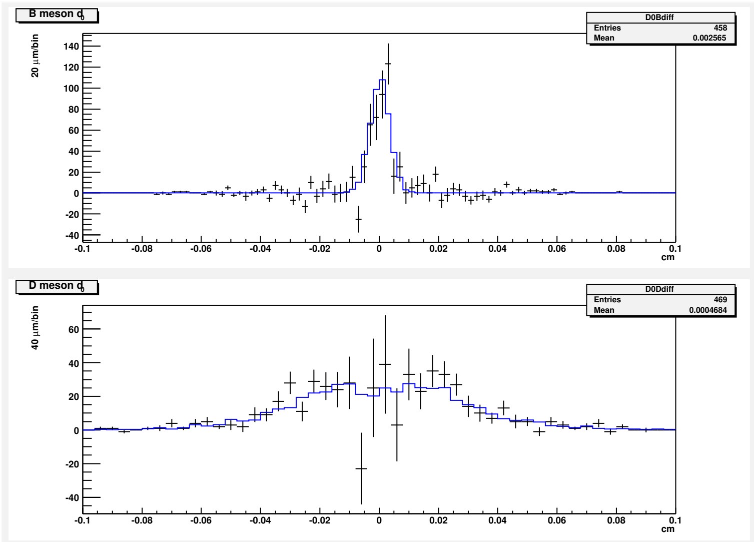

Figure 13: Comparison between Monte Carlo simulation and Data.

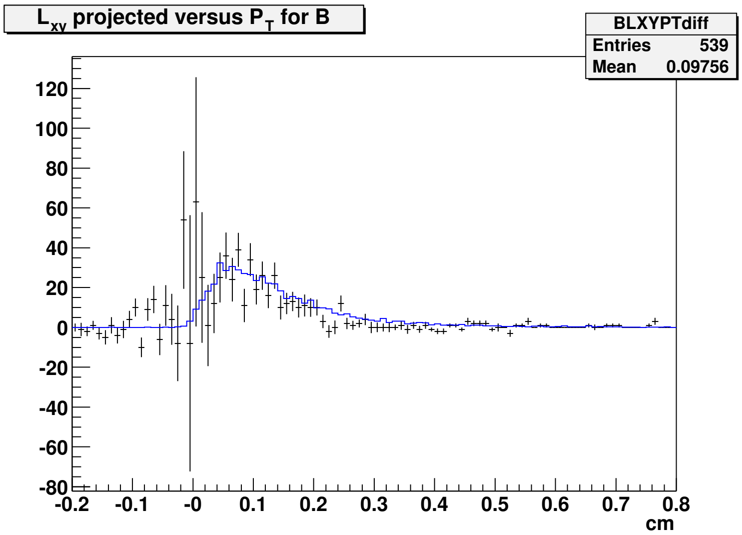

Figure 14: Comparison between Monte Carlo simulation and Data.

mesons impact parameter distributions, reported in figure 13 and by the B and D mesons decay lengths, fig. 14.

In table 6 the efficiencies for all the simulated runs and all the decays used are reported. The table shows a behavior consistent with the properties of the run ranges which each run represents, in terms of improvements and losses in efficiency. The overall efficiency we use in the extraction of the relative yield is an average of each of

run	$B_s(\phi\pi)(\%)$	$B_u(D^0\pi)(\%)$	$B_d(K\pi\pi)(\%)$
141508	1.02±0.03	1.30±0.03	1.11±0.03
144578	1.00±0.03	1.14±0.03	1.03±0.03
146920	1.01±0.02	1.23±0.02	1.14±0.02
150003	1.34±0.03	1.65±0.04	1.48±0.03
150799	1.28±0.03	1.58±0.04	1.48±0.03
151513	1.37±0.02	1.57±0.03	1.51±0.02
152747	1.48±0.03	1.72±0.05	1.62±0.03
153618	1.51±0.02	1.80±0.02	1.71±0.02
Weighted Average	1.360±0.008	1.620±0.010	1.524±0.009

Table 6: Trigger efficiency for different runs.

the above efficiencies weighted proportionally to the luminosity integrated in data for each of run periods (see table 5): $\epsilon = \sum L_i/L_{tot}\epsilon_i$.

Since in the reconstruction we require a minimum number of axial hits in the silicon for each track, we have to evaluate this efficiency as a function of the period the data has been taken: we do that for each run range and then quote a luminosity weighted efficiency. The results of this study are summarized in table 7.

The analysis cuts on the transverse momentum, the L_{xy} the χ^2 and the impact

run	$B_s(\phi\pi)(\%)$	$B_u(D^0\pi)(\%)$	$B_d(K\pi\pi)(\%)$
141508	51±1	54±1	44±1
144578	40±1	44±1	35±1
146920	50±1	54±1	43±1
150003	47±1	51±1	41±1
150799	55±1	55±1	44±1
151513	46±1	50±1	40±1
152747	48±1	49±1	39±1
153618	46±1	47±1	39±1
Weighted Average	45.0± 0.3	47.2± 0.3	39.7±0.3

Table 7: Reconstruction efficiency for different runs.

parameter have different efficiencies on different decays but they do not depend on the detector configuration anymore. We can therefore safely evaluate their efficiency without luminosity weighting. The results are summarized in table 8.

Since we are interested in evaluating the ratio of the number of events seen in different

	$B_s(\phi\pi)(\%)$	$B_u(D^0\pi)(\%)$	$B_d(K\pi\pi)(\%)$
ϵ_{ANA}	58.2 $\pm$ 0.7	49.2 $\pm$ 0.6	54.1$\pm$ 0.8

Table 8: Analysis cuts efficiency.

channels, what really matters are the ratios of efficiencies between the different modes. These are reported in table 9. The quoted error is statistical but it includes the systematic effects coming from the partial coverage of the silicon and the changes in svtsim pattern and constants for the different periods of data taking.

	B_s/B_d	B_d/B_u
$\epsilon_{Trigger}$	0.892$\pm$0.008	0.941$\pm$ 0.008
ϵ_{Reco}	1.134$\pm$0.012	0.841$\pm$0.011
ϵ_{Ana}	1.07 $\pm$0.02	1.10$\pm$ 0.02
ϵ_{tot}	1.08 $\pm$0.02	0.87$\pm$0.02

Table 9: Ratio of efficiencies for all the decay used.

6.2 Systematic Errors

Before using the efficiencies found with the Monte Carlo we perform several checks and evaluate the systematic errors on the ratio.

The first systematic we check is the bias introduced by the generation cuts. The same ratios, exactly with the same procedure, have been evaluated in samples of events generated with a minimum b momentum at zero. A comparison between these new numbers and the ones obtained previously is reported in table 10: generating B with a minimum P_t at 5.5 GeV appears safe enough for all the decays we are using. The residual discrepancy is included as systematic error. Another significant variation on

	B_s/B_d	B_d/B_u
Ratio ($P_{min} = 0$)	1.16$\pm$0.03	0.87$\pm$0.02
Ratio ($P_{min} = 5.5$)	1.08$\pm$0.02	0.76$\pm$0.02
($P_{min} = 5.5$)- ($P_{min} = 0$)	-0.08$\pm$0.04	-0.11$\pm$0.04

Table 10: Ratio of efficiencies for all the decay with two different minimum b quark momenta.

the efficiencies ratios can come from the uncertainty on the lifetimes of the B and

D mesons. This variation is evaluated in a conservative way, by varying by $+1\sigma$ the lifetime of B_s and -1σ that of the B_d, evaluating the ratio, and comparing this to the one we obtain when we vary by -1σ the lifetime of the B_s and -1σ the B_d. The same procedure is followed for the D_s and $D^{\pm}$. In table 11 we report the efficiency ratios with the varied lifetime.

	B_s/B_d
B^{num} up B^{den} down	1.12±0.01
B^{num} down B^{den} up	1.06±0.02
D^{num} up D^{den} down	1.12±0.02
D^{num} down D^{den} up	1.08±0.02

Table 11: Ratio of efficiencies for all the decay with the B and D lifetime varied as described in the text.

Another potential systematic variation in the efficiency ratio can come from the presence of several trigger paths besides the *scenario A*, with different prescales. At the moment when we select the `B_CHARM`path we are accepting all the incarnations of the hadronic trigger, namely the so called scenario A, B, C and the low pt with different dynamic prescales.
In particular the latter can give significantly different relative efficiencies since it does not include the opposite charge cut and the sum Pt cut.
Our simulation emulates only one path at a time, and we decided to stick to the scenario A taking into account for the residual difference when including the low Pt part of the sample.
We studied the variation in the efficiency ratio, but then we then decided not to include these events in our measurement since at the moment it is difficult to get a reliable evaluation of the number of volunteers coming through this prescaled path. For future reference we report here the results of the study.

In table 12 we compare the results in term of trigger efficiency for the two scenarios, while in table 13 the variation in the ratio is summarized. The ratio seems is not

	$B_s(\phi\pi)(\%)$	$B_d(K\pi\pi)(\%)$
$ScenarioA$	0.45± 0.01	0.53± 0.01
$LowPt$	0.73± 0.01	0.88± 0.01

Table 12: Absolute trigger efficiency for two different trigger scenarios: A and low Pt.

strongly dependent on the trigger setup therefore we plan to include the additional events in a future measurement.

The last systematics we check is still trigger related: our simulation assumes that the XFT was always configured in the “2 miss” mode, while part of the data has been taken with the “1 miss”requirement. This introduces a bias in our efficiency ratio that we measure by generating one of the last two runs of table 5 with the XFT 1-miss configuration and calculating the change in the efficiency ratio. The global shift is 0.001 ± 0.047 for the B_s/B_d ratio and 0.04 ± 0.047 for B_d/B_u. An additional correction woudl come then from the fact that the XFT efficiency in the “1 miss” configuration has an η dependancy which is not reproduced by the simulation. This tracking efficiency goes more or less like $|\eta| \cdot 0.1 + 0.9$. When applying this in a parametrized fashion ontop of the “1 miss” simulated run we find no significant difference in the relative efficiencies.

We summarize in table 14 all the significant systematic errors.

	B_s/B_d
Ratio (scenario A)	0.85±0.02
Ratio (Low Pt)	083±0.01
(Scenario A)- (Low Pt)	0.02±0.02

Table 13: Ratio of efficiencies for all the decays for 2 different trigger scenario.

	B_s/B_d	
1-miss		+0.001
Minimum b quark P_t	-0.08	—-
B lifetimes	-0.02	+0.04
D lifetimes	0.00	+0.04
Total	-0.08	+0.06

Table 14: Summary of all systematic errors on the ratio of efficiencies.

7 Conclusions

7.1 B_d and B_u relative yield

Now we have all the ingredients to measure the relative yields. First of all we check our procedure by comparing the B_d/B_u relative yield seen in the data with the MC predictions:

$$\frac{N_{B_d}}{N_{B_u}} = \frac{\epsilon_{B_d}}{\epsilon_{B_u}} \frac{Br(B_d \to D\pi)Br(D \to k\pi\pi)}{Br(B_u \to D^0\pi)Br(D^0 \to K\pi))}$$

From the PDG we get $\frac{Br(B_d \to D\pi)Br(D \to k\pi\pi)}{Br(B_u \to D^0\pi)Br(D^0 \to K\pi)} = 1.36 \pm 0.24$ and by using the simulation we obtain $\frac{\epsilon_{B_d}}{\epsilon_{B_u}} = 0.87 \pm 0.02$ which gives an expected ratio of $\frac{N_{B_d}}{N_{B_u}} = 1.18 \pm 0.21$. In the data we measure $\frac{N_{B_d}}{N_{B_u}} = 1.04 \pm 0.13$ which is in good agreement with the expectations.

7.2 B_s relative yield

We finally use the Monte Carlo efficiency to correct the data and estimate the B_s/B_d relative yield. Following the same procedure:

$$\frac{N_{B_s}}{N_{B_d}} = \frac{f_s}{f_d} \frac{\epsilon_{B_s}}{\epsilon_{B_d}} \frac{Br(B_s \to D_s\pi)Br(D_s \to \phi\pi)Br(\phi \to kk)}{Br(B_d \to D\pi)Br(D \to k\pi\pi)}$$

The simulation predicts $\frac{\epsilon_{B_s}}{\epsilon_{B_d}} = 1.08 \pm 0.02\ ^{+0.06}_{-0.08}$ while from PDG we obtain $\frac{Br(D_s \to \phi\pi)Br(\phi \to kk)}{Br(D \to k\pi\pi)} = 0.19 \pm 0.05$.

On data we measure $\frac{N_{B_s}}{N_{B_d}} = 0.087 \pm 0.023$. The error here is only statistical and we assign a systematic error to the number of events for the uncertainty on the fit function and the fit range. The maximum variation we observed was 10%, which yields: $\frac{N_{B_s}}{N_{B_d}} = 0.087 \pm 0.023 \pm 0.008(B_s fit) \pm 0.008(B_d fit)$. The ratio of the number of events is then corrected by the efficiency ratio and divided by the know branching ratios taken from PDG to obtain:

$$\frac{f_s}{f_d} \frac{Br(B_s \to D_s\pi)}{Br(B_d \to D\pi)} = 0.42 \pm 0.11(stat.) \pm 0.11(BR) \pm 0.07(syst.)$$

This is our preliminary result, with a rather conservative approach for the systematics evaluation.

References

[1] *CDF Note 5134*.

[2] "The CharmMods/DFinder Reconstruction Package" S. Giagu *CDF Note 6158*.

[3] Stefano Giagu: private communication.

[4] The Trigger and Dataset Working Group: "Run-II Trigger Table and Datasets Plan" *CDF Note 4718*.

[5] A. Cerri: "Survey of CP-violating B_u, B_d fully hadronic decays accessible in Run II", *CDF Note 5243*.

[6] "B Physics at the Tevatron: Run II and Beyond", *FERMILAB-PUB-01/197*.

[7] I.Furic, C. Paus " Event Yield Estimates for Hadronic B_s Decays in Run II" *CDF Note 5349*